

NEANDC ( OR ) - 157 " U "

INDC ( SWT ) - 16 / L

PROGRESS REPORT  
TO INDC AND NEANDC  
FROM SWITZERLAND

June 1982

F. Widder

Swiss Federal Institute for Reactor Research  
Würenlingen

~~NOT FOR PUBLICATION~~

## PREFACE

This document contains information of a preliminary or private nature and must be used with discretion. Its contents may not be quoted, abstracted, reproduced, transmitted to libraries or societies or formally referred to without the explicit permission of the originator.

## CONTENTS

I.	Institut de Physique, Université de Neuchâtel	1
II.	Laboratorium für Kernphysik der ETH Zürich	6
III.	Eidg. Institut für Reaktorforschung, Würenlingen	20

I. Institut de Physique, Université de Neuchâtel

---

1. Elastic proton-proton scattering at  $90^\circ$ CM between  
500 and 600 MeV

P. Chatelain, B. Favier, F. Foroughi, J. Piffaretti

During the study [1] of pion production in the reaction  $pp \rightarrow \pi d$  the elastic  $pp$  scattering was used for normalization. Since for proton energies between 500 and 600 MeV published elastic  $pp$  differential cross section data were scarce and not all in agreement, we evaluated this cross section  $\sigma(90^\circ)$  for  $90^\circ$ CM for seven energies between 516 and 582 MeV.

The experiment was performed at the PM1 secondary beam line of SIN. To avoid the influence of the proton polarization due to the  $8^\circ$  scattering of the primary beam (592 MeV protons) by the thin production target (Be), the proton polarization was rotated from the vertical to an horizontal direction using a superconducting solenoid. Additional suppression of polarization effects is due to vanishing analyzing power for  $pp$  elastic scattering at  $90^\circ$ .

The experimental set-up is shown in fig. 1. We used a small  $\text{CH}_2$  target ( $10 \times 10 \times 5 \text{ mm}^3$ ). The protons from  $pp$  scattering were detected in coincidence in two telescopes P1 and P2. The coincidence counting rate between D2 and D3 gives the number of particles per sec in the incident beam. The fraction  $\eta$  of the incident beam hitting the target and the transmission factors ( $\omega_t$  and  $\omega_d$ ) of the  $\text{CH}_2$  target and the detectors were determined also.

All detectors were NE 102A plastic scintillators 5 mm thick. The single and appropriate coincident counting rates were recorded on magnetic tape every 10 sec, thus producing an history of the experiment.

The mean energy  $E_p$  of the incident protons was varied using copper absorbers.  $E_p$  has been determined within  $\pm 1.5$  MeV [1]. The beam intensity  $R_0$  was reduced to about 0.2 protons per 51 MHz burst, requiring the use of Poisson statistics in data analysis.

To find the fraction  $\eta$  of  $R_0$  hitting the target, it was replaced by a detector D1 of equal size.  $\eta$  and the transmission  $\omega_d$  for 5 mm NE102A scintillator was obtained from coincident rates between D1, D2 and D3.  $\eta$  varied from  $0.862 \pm 0.004$  at 582 MeV to  $0.776 \pm 0.003$  at 516 MeV due to decreasing beam quality. No significant energy dependence of  $\omega_d$  was observed, the mean value being  $\omega_d = 1 - (12 \pm 1) \cdot 10^{-3}$ .

To determine the transmission  $\omega_t$  of the target material (5 mm  $\text{CH}_2$ ) an appropriate  $\text{CH}_2$  sheet was inserted between detectors D2 and D3. It was found to be  $\omega_z = 1 - (8 \pm 1) \cdot 10^{-3}$  over the entire energy range.

The pp elastic differential cross section  $\sigma(90^\circ)$  was deduced from the ratio of coincident counting rates in the telescopes P1 and P2 and the intensity  $\eta R_0$  of the beam hitting the target. A more detailed description of the experiment is given in ref. 2.

Our results are plotted in fig. 2 (full circles). The error bars include the statistical errors of telescope counting rates, uncertainties of the above mentioned corrections, of the target thickness ( $\pm 1\%$ ), of the reaction losses ( $\pm 0.5\%$ ) in the detectors P1 and P2, and of background due to carbon ( $\pm 1\%$ ). Our values are slightly higher than a phase shift prediction by BUGG [3] and differ significantly from the results [3-7] of previous experiments.

## References

- {1} J. Hoftiezer, Ch. Weddigen, B. Favier, S. Jaccard, P. Walden, P. Chatelain, F. Foroughi, C. Nussbaum and J. Piffaretti  
Phys. Lett. 100 B(1981)462
- {2} P. Chatelain, B. Favier, F. Foroughi, J. Hoftiezer, S. Jaccard, J. Piffaretti, P. Walden and Ch. Weddigen  
to be published in Journal of Phys. G Nuclear phys. 8 (1982)
- {3} D.V. Bugg, private communication (1979)
- {4} M.G. Mescheriakov, B.S. Neganov, L.M. Soroko and J.K. Vzorov  
Doklady Akad. Nauk. SSSR 99(1954)959
- {5} E.T. Boschitz, W.K. Roberts, J.S. Vincent, H. Blecher, K. Gotow, P.C. Gugelot, C.F. Perdrisat, L.W. Swensen and J.R. Priest  
Phys. Rev. C6(1972)457
- {6} L.W. Smith, W.A. Mc Kengold and G. Snow  
Phys. Rev. 97(1955)1186
- {7} S.J. Nikitin, J.M. Selector, E.G. Bogomolov and S.M. Zomporoskij  
Nuovo Cimento 2(1955)1269

## Figure captions

Fig. 1: Schematic representation of the experimental set-up.

Detector D1 serves to determine the fraction  $\eta$  of the incident beam  $R_0$  hitting the target.  $R_0$  is submitted by coincidences between D2 and D3. For differential cross section measurements, detector D1 is replaced by a  $\text{CH}_2$  target and pp coincidences are detected by the telescopes P1 and P2. The  $\text{CH}_2$  absorber between detectors D2 and D3 is inserted to determine the reaction losses in  $\text{CH}_2$ . Transmissions are denoted by  $\omega$ .

Fig. 2: Comparison of our experimental results (full circles) for the CM differential cross section  $\sigma(90^\circ)$  of elastic pp scattering with a phase shift prediction by BUGG {3} (curves) and with experimental results of MESCHERIAKOV et al. {4} (open circles), of BOSCHITZ et al. {5} (full square), of SMITH et al. {6} (open square), and of NIKITIN et al. {7} (triangle).  $E_p$  = proton kinetic lab. energy.

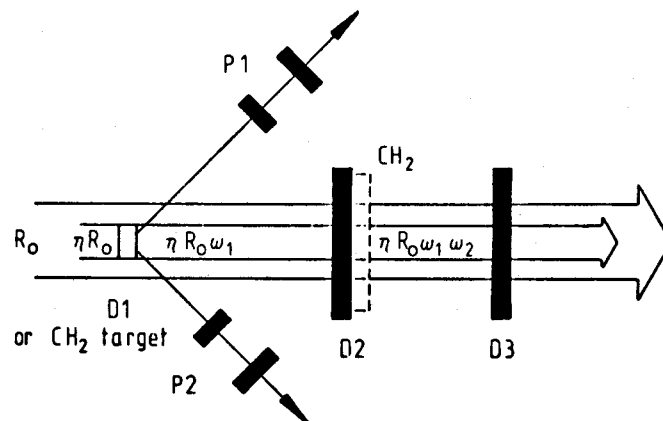


Figure 1

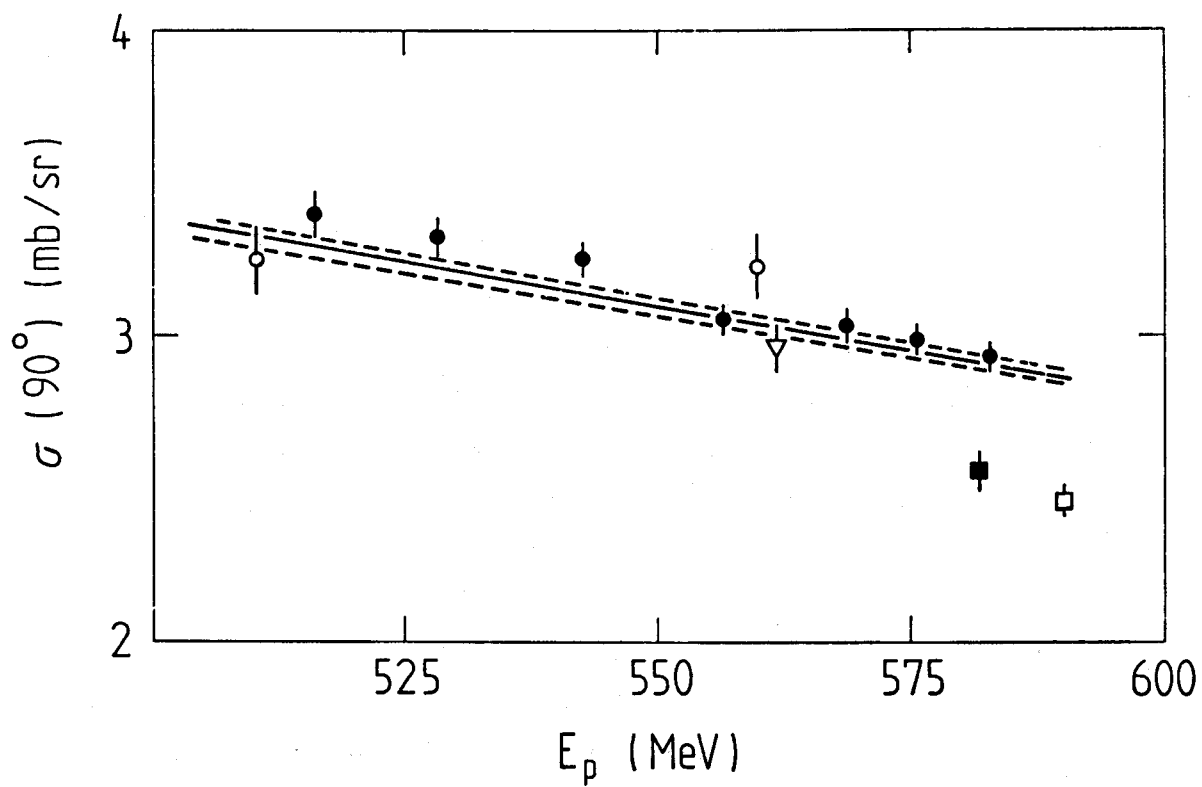


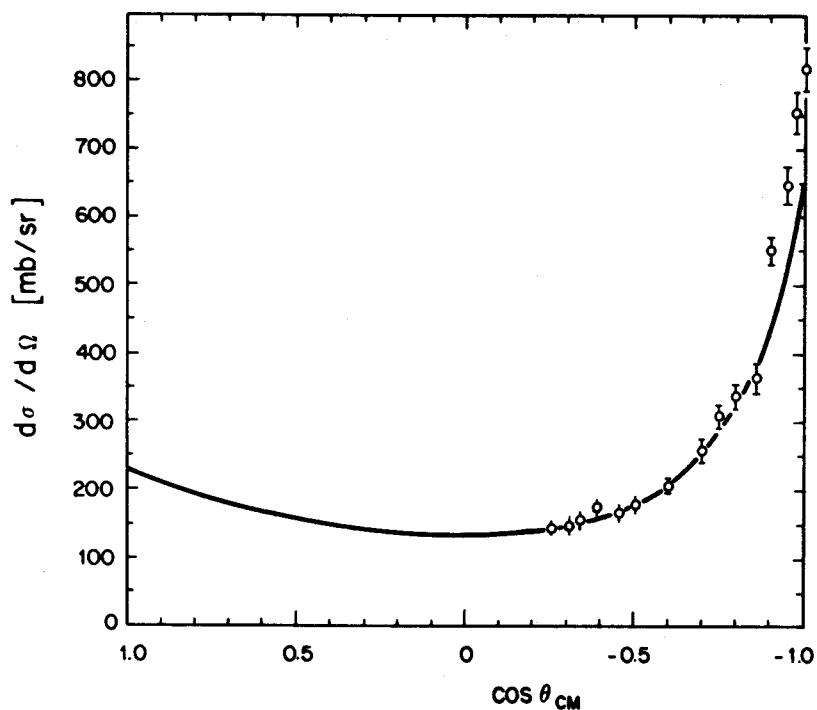
Figure 2

2. The (n,d) differential elastic cross section at 2 MeV

J. Weber

The (n,d) differential elastic cross section at 2.016 MeV has been measured in the  $104^\circ$  to  $180^\circ$  angular range (CM). The results have been accepted for publication in *Helv. Phys. Acta*. The present data, beyond  $140^\circ$ CM, are larger than earlier data; this is discussed, in the paper, in view of some theoretical predictions.

A sample of our data is shown in the following figure (circles: experimental results/curve: Goldberg et al., BNL 400, 2nd Ed., Vol. I).



The same cross section is currently being measured at 3 MeV. This will complete our set of measurements (cross section, polarization and depolarization) of (n,d) elastic scattering below the breakup threshold.

It is already apparent that the neutron depolarization data {1} cannot be fitted unless the 2 S and 2 P phase shifts are respectively smaller and larger than the values predicted by 3-body calculations.

{1} D. Bovet et al., Progress Report to NEANDC from Switzerland, 1979.

II. Laboratorium für Kernphysik der ETH Zürich

1. New highly excited  $^4\text{He}$  levels found by the  $^2\text{H}(\vec{d},p)^3\text{H}$  reaction

W. Grüebler, V. König, P.A. Schmelzbach, B. Jenny and  
J. Vybiral

The differential cross section, the vector- and the tensor-analyzing powers of the reaction  $^2\text{H}(\vec{d},p)^3\text{H}$  have been measured. The polarization data were obtained at 11 energies between 1.0 and 13 MeV at lab. angles between  $5^\circ$  and  $160^\circ$ . The data were fitted with Legendre polynomials and the resulting coefficients analyzed for resonances in  $^4\text{He}$ . Overwhelming evidence for a  $1^-$  level at 24.1 MeV and a strong indication of a  $4^+$  level at 24.6 MeV excitation energy have been found. The experimental results are shown in fig. 1 to 3 and the coefficients found in the Legendre polynomial analysis in fig. 4 and 5.



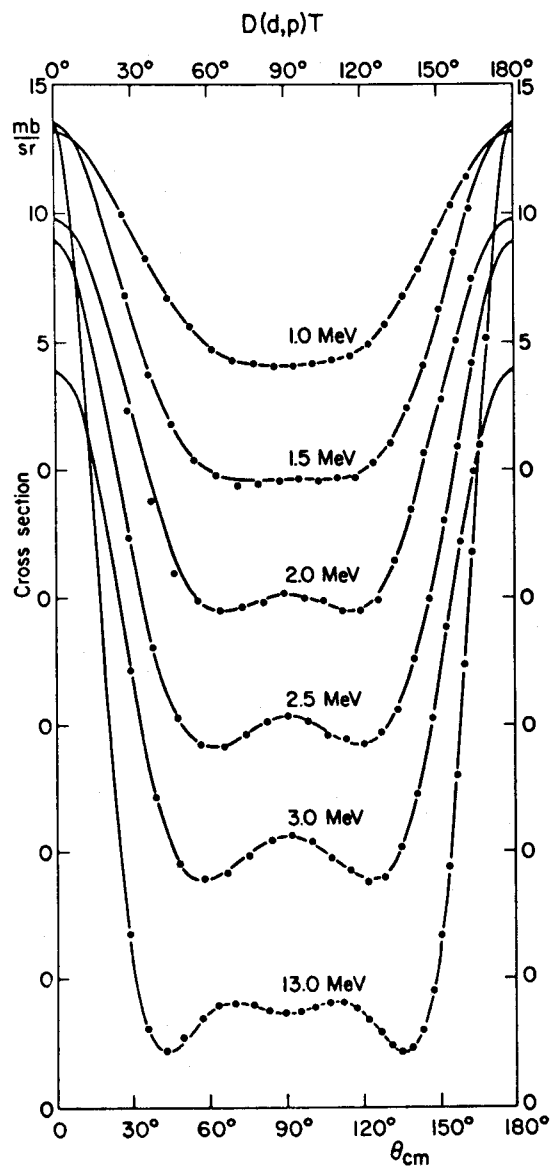


Fig. 1 Angular distributions of the cross section for the  ${}^2\text{H}(d,p){}^3\text{H}$  reaction. The dots are larger than the statistical error. The solid lines are Legendre polynomial fits

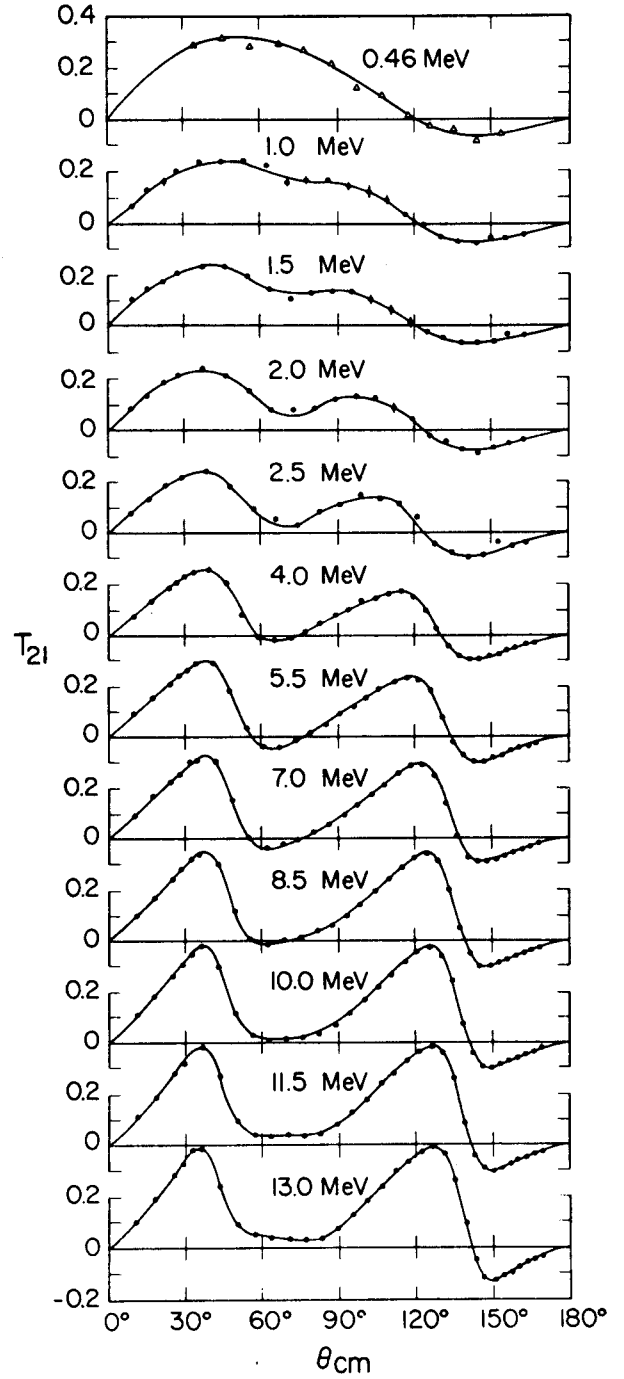
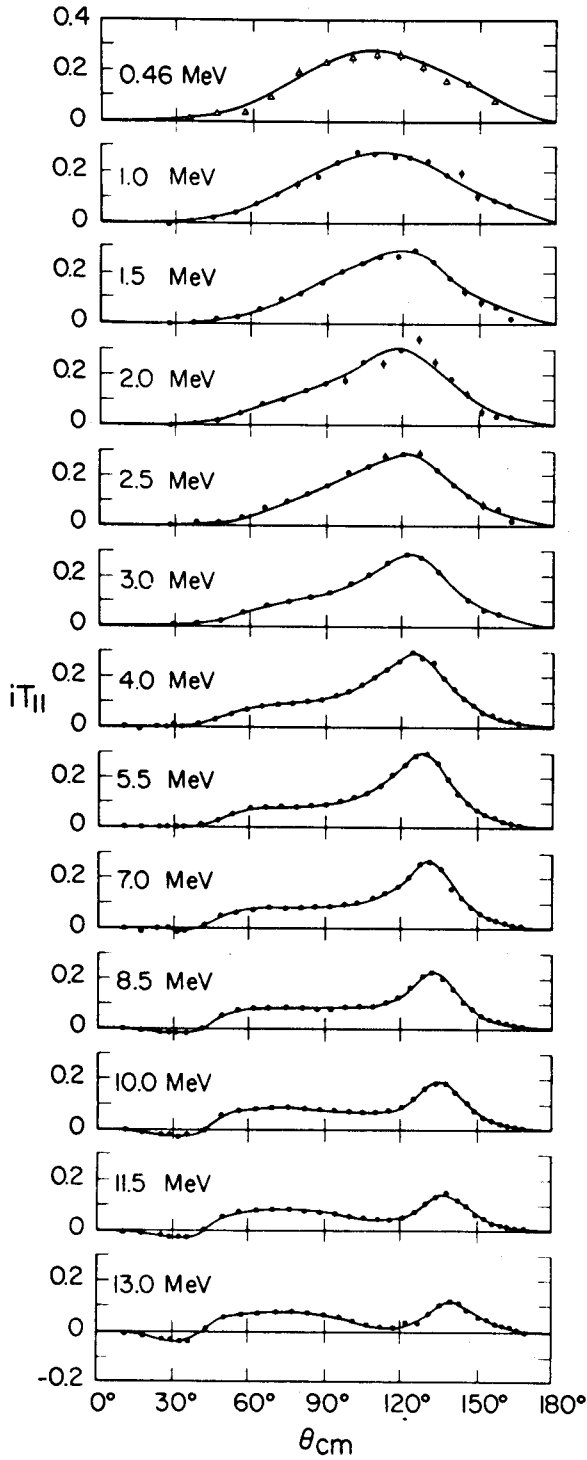


Fig. 2 The analysing powers  $iT_{11}$  and  $T_{21}$  between 0.46 and 13.0 MeV. Where no error bars are shown the statistical error is smaller than the dots. The solid lines are Legendre polynomials fits

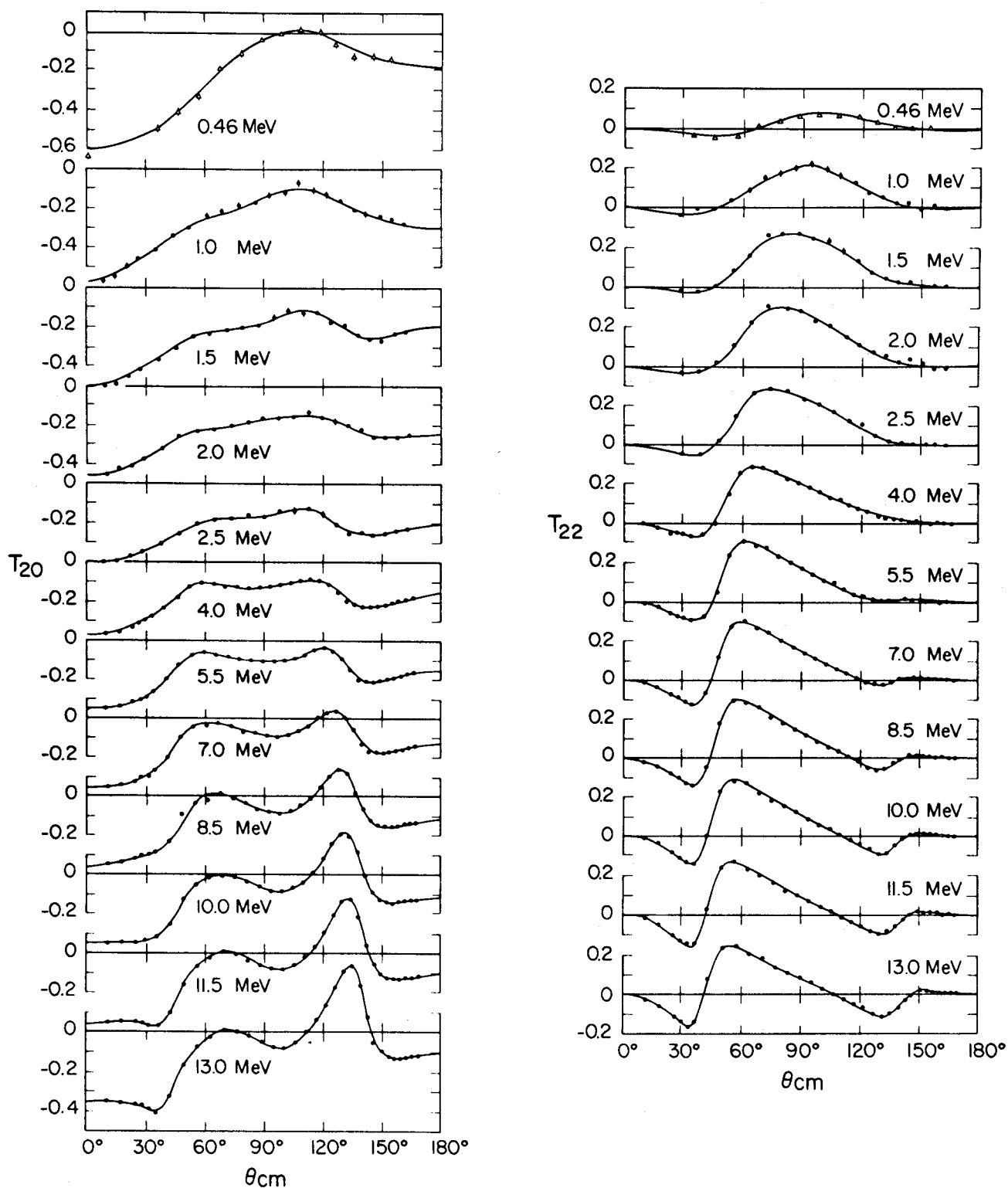


Fig. 3 The tensor analysing powers  $T_{20}$  and  $T_{22}$  between 0.46 and 13.0 MeV. Where no error bars are shown the statistical error is smaller than the dots. The solid lines are Legendre polynomial fits

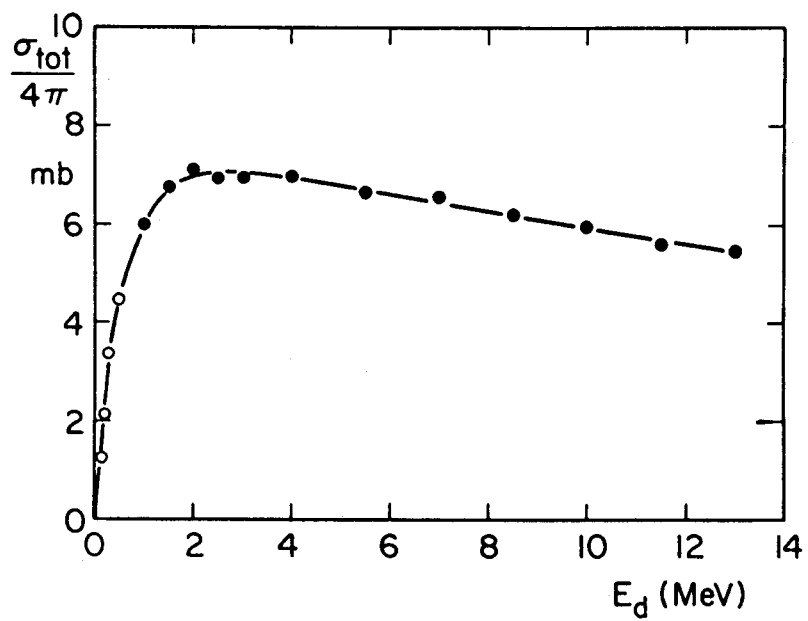


Fig. 4 Total cross section  $\sigma_T/4\pi$  of the  $^2\text{H}(d,p)^3\text{H}$  reaction

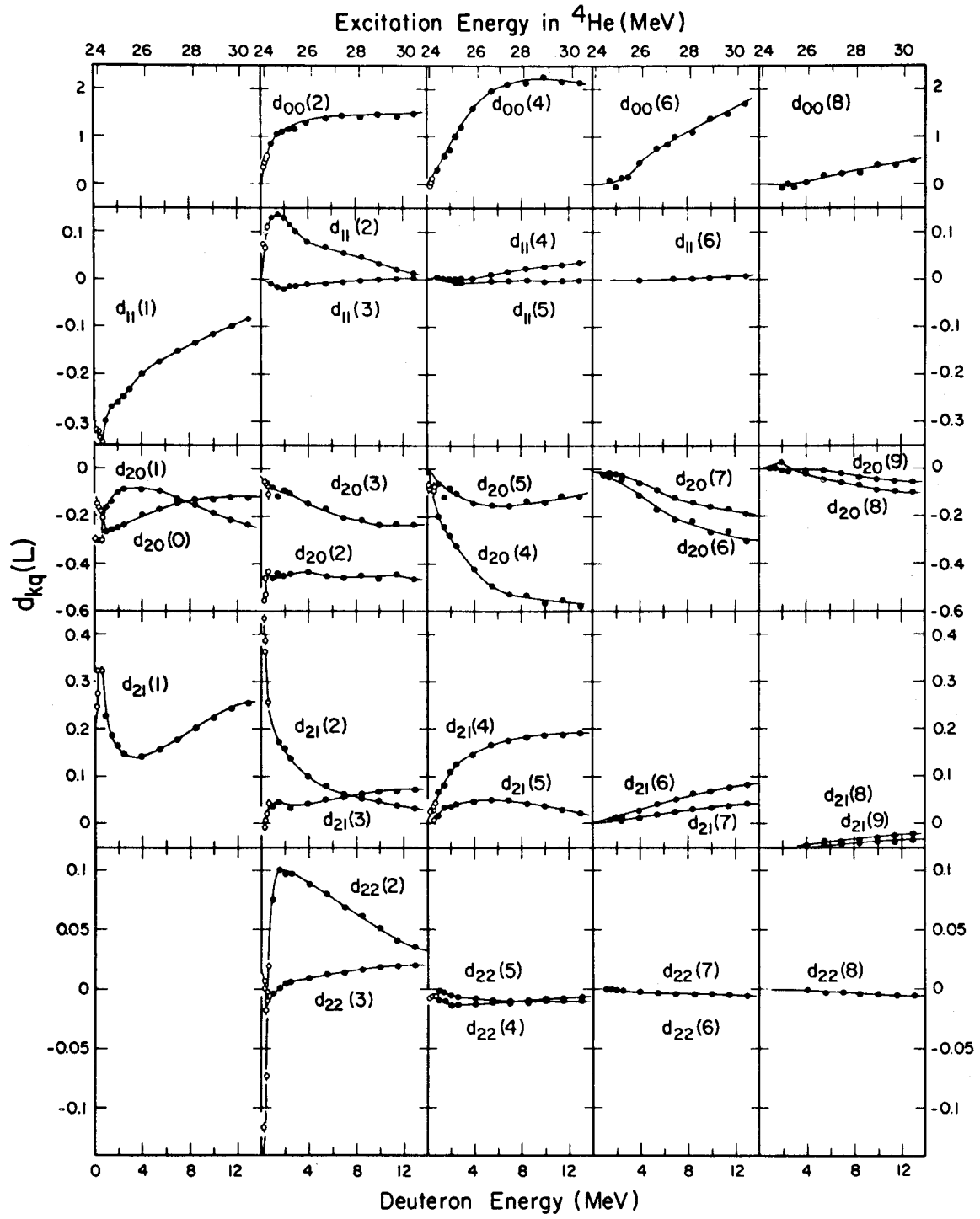


Fig. 5 Normalized Legendre polynomial expansion coefficients  $d_{kq}(L)$  for the differential cross section and the vector and tensor analysing powers. The dots are larger than the uncertainties of the fits

2. Evidence for N-N off-shell effects in the polarization transfer coefficients of p-d elastic scattering

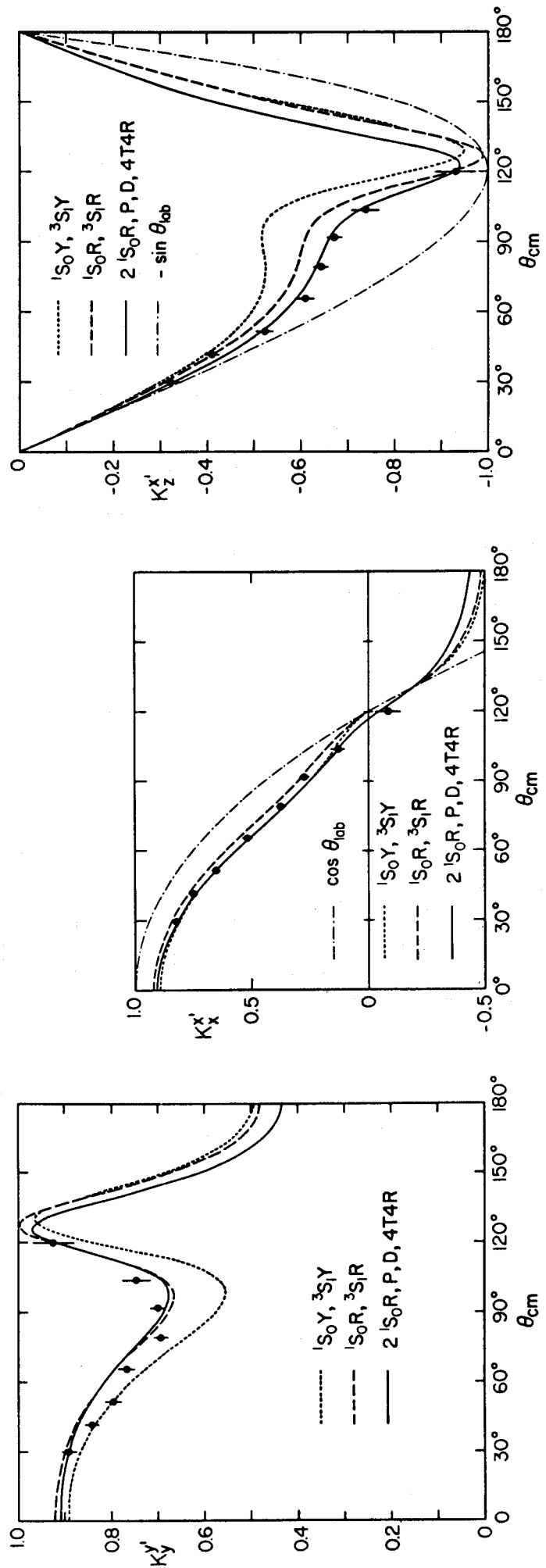
F. Sperisen, W. Grüebler, V. König, P.A. Schmelzbach,  
B. Jenny, K. Elsener, C. Schweizer and J. Ulbricht

Measurements of the polarization transfer coefficients  $K_y^{y'}$ ,  $K_x^{x'}$  and  $K_z^{x'}$  for the  ${}^2\text{H}(\vec{p}, \vec{p}) {}^2\text{H}$  elastic scattering at  $E_p = 10$  MeV are reported in the angular range between  $\theta_{\text{cm}} = 30^\circ$  and  $120^\circ$ . These second order polarization observables are compared with Faddeev calculations. They depend largely on the details of the S-wave interactions and the results are sensitive to the choice of their formfactors, i.e. to properties of the off-shell behaviour.

Reference

F. Sperisen et al., Phys. Lett. 102 B (1981) 9.

Figure: The polarization transfer coefficients  $K_y^{y'}$ ,  $K_x^{x'}$  and  $K_z^{z'}$ . The dotted curve is a S-wave calculation with a Yamaguchi formfactor, the dashed curve with a short range repulsion and the solid curve a full Faddeev calculation. The dashed-dotted curve represents a kinematical rotation



3. Production of intense beams of polarized negative hydrogen ions by the atomic beam method

P.A. Schmelzbach, W. Grüebler, V. König and B. Jenny

The production of a 3  $\mu$ A polarized negative hydrogen ion beam by the ETH atomic beam type polarized ion source is described in [1]. After acceleration in a tandem accelerator a record current of 1.6  $\mu$ A of polarized deuterons with 89% polarization could be focused through a 3 mm diameter collimator on a target. Recently it could be shown that it is possible to obtain 50-100  $\mu$ A of polarized  $H^-$  and  $D^-$  ions with this type of source by means of further improvements incorporating presently available techniques.

Reference

[1] P.A. Schmelzbach et al., Nucl. Instr. and Meth. 186 (1981)655.

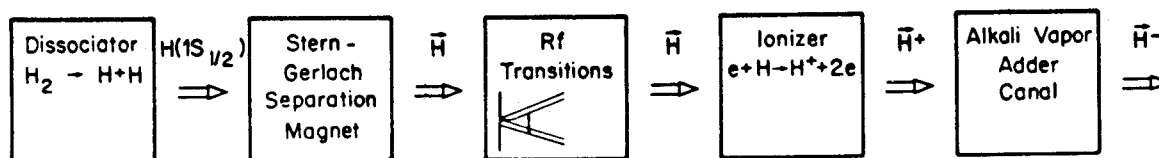


Fig. 1 Schematic diagram of the atomic beam source for polarized negative hydrogen ions



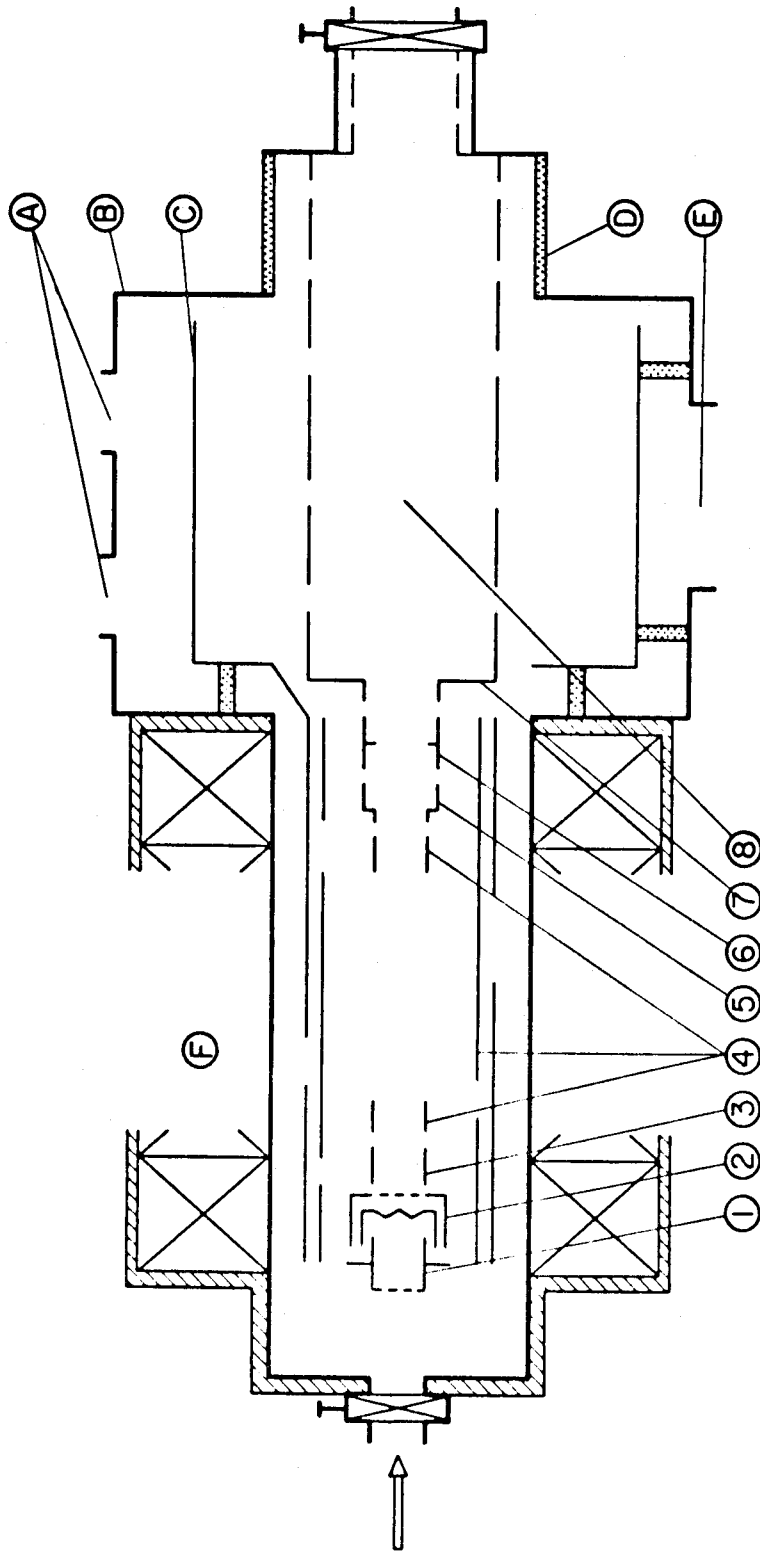


Fig. 2 Schematic representation of the ETH ionizer (not to scale)

General: A: pumping ports (two 900  $\ell$ /sec orbitron pumps),

B: vacuum housing, C: electrode supporting system, D: insulator,

E: pumping port (5000  $\ell$ /sec  $\text{LN}_2$ -baffled diffusion pump),

F: solenoid coil. Electrode system: 1: electron repelling,

2: filament and grid, 3: electron acceleration and ion

repelling, 4: ionisation column potential, 5: electron

reflexion and ion extraction, 6: preacceleration,

7-8: acceleration, beam forming and transport to charge exchanger

#### 4. Radioisotope dating with an EN tandem accelerator

R. Balzer, G. Bonani, Ch. Stoller, M. Suter and W. Wölfli

The EN tandem facility at the ETH Zürich was modified for routine dating of small C and Be samples. The system shown in Fig. 1 consists of a Cs sputter ion source with a  $90^\circ$  inflection magnet at the low energy side and a combination of an electrostatic deflection plates,  $90^\circ$ -analyzing magnet and  $\Delta E$ -E counter telescope at the high energy side.

The sputter ion source is designed for low cross contamination between specimens and convenient loading of samples. Up to 25 samples can be loaded into the vacuum box during full operation of the ion source and each specimen can be placed to the sputter position automatically when requested by the computer. The ion source delivers  $10\text{--}30\ \mu\text{A}$   $^{12}\text{C}$  beams. This allows to date modern C-samples with a statistical accuracy of better than 1% within a few minutes. A whole series of samples can be measured automatically in a preprogrammed sequence. The various isotopes of a sample are injected sequentially into the accelerator. First the inflection magnet is set on the rare isotope and then the more abundant isotopes are injected periodically ( $\sim 20\text{ Hz}$ ) during about  $200\ \mu\text{s}$  by applying high voltage pulses to the insulated vacuum chamber of this magnet. The measurement of each sample is divided into intervals of 20–60 s duration, for which the data are analyzed and compared with the results of previous intervals. Details of the pulsing technique and the computer controlled system are described elsewhere [1,2].

Fig. 2 shows a typical particle spectrum obtained from a modern carbon sample. The accelerator was set at a voltage of 4.5 MV and the particles recorded with the  $\Delta E$ -E heavy ion detector had an energy of 22 MeV and charge state  $3^+$ . Only two well separated peaks are visible, which can be assigned to  $^{14}\text{C}$  and  $^{14}\text{N}$ . The  $^{14}\text{N}$  particles are fragments of  $^{14}\text{N H}^-$  molecules which were able to pass through all mass and energy filters. The background level is low and  $^{14}\text{C}/^{12}\text{C}$  ratios with a sensitivity of at least  $5 \cdot 10^{-16}$  can be measured. This corresponds to an apparent age of about 65'000 y for carbon. These ratios can

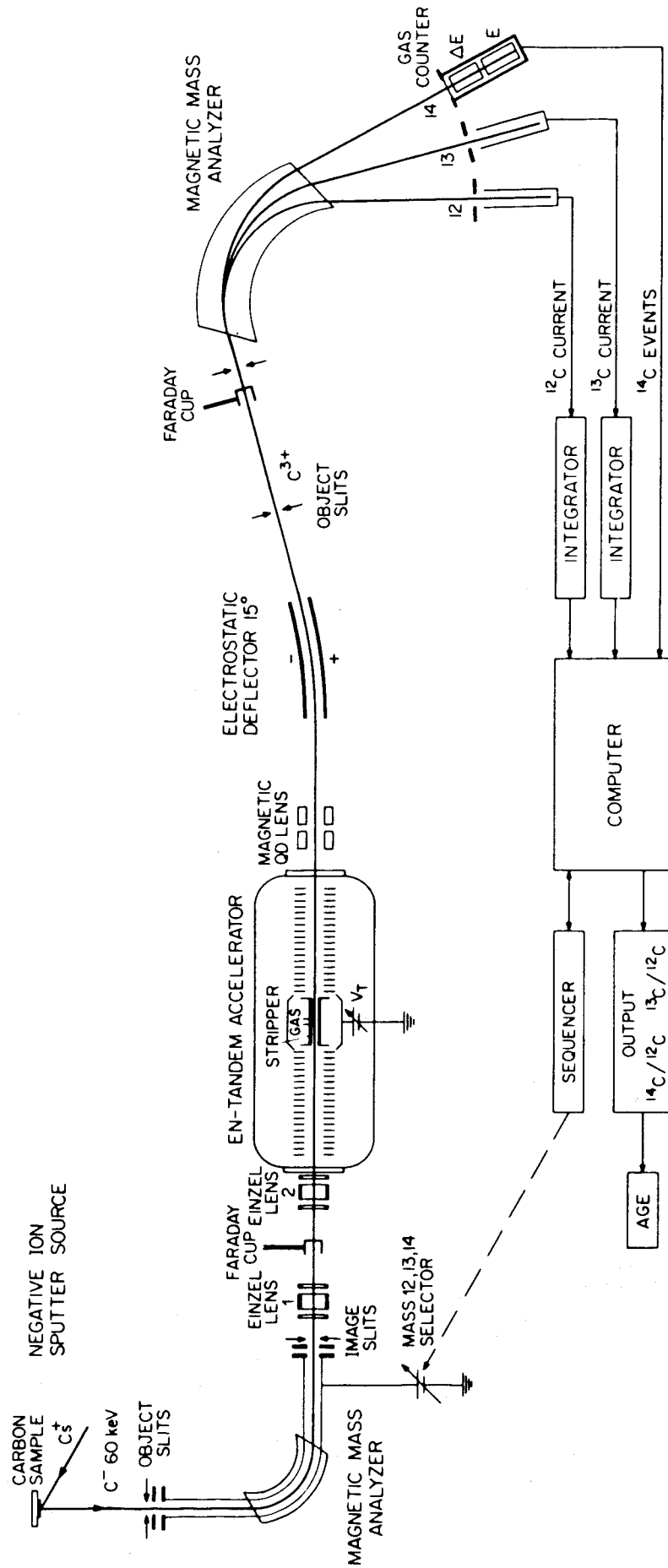


Fig. 1 Schematic diagram of the ETH Tandem Van de Graaff dating facility

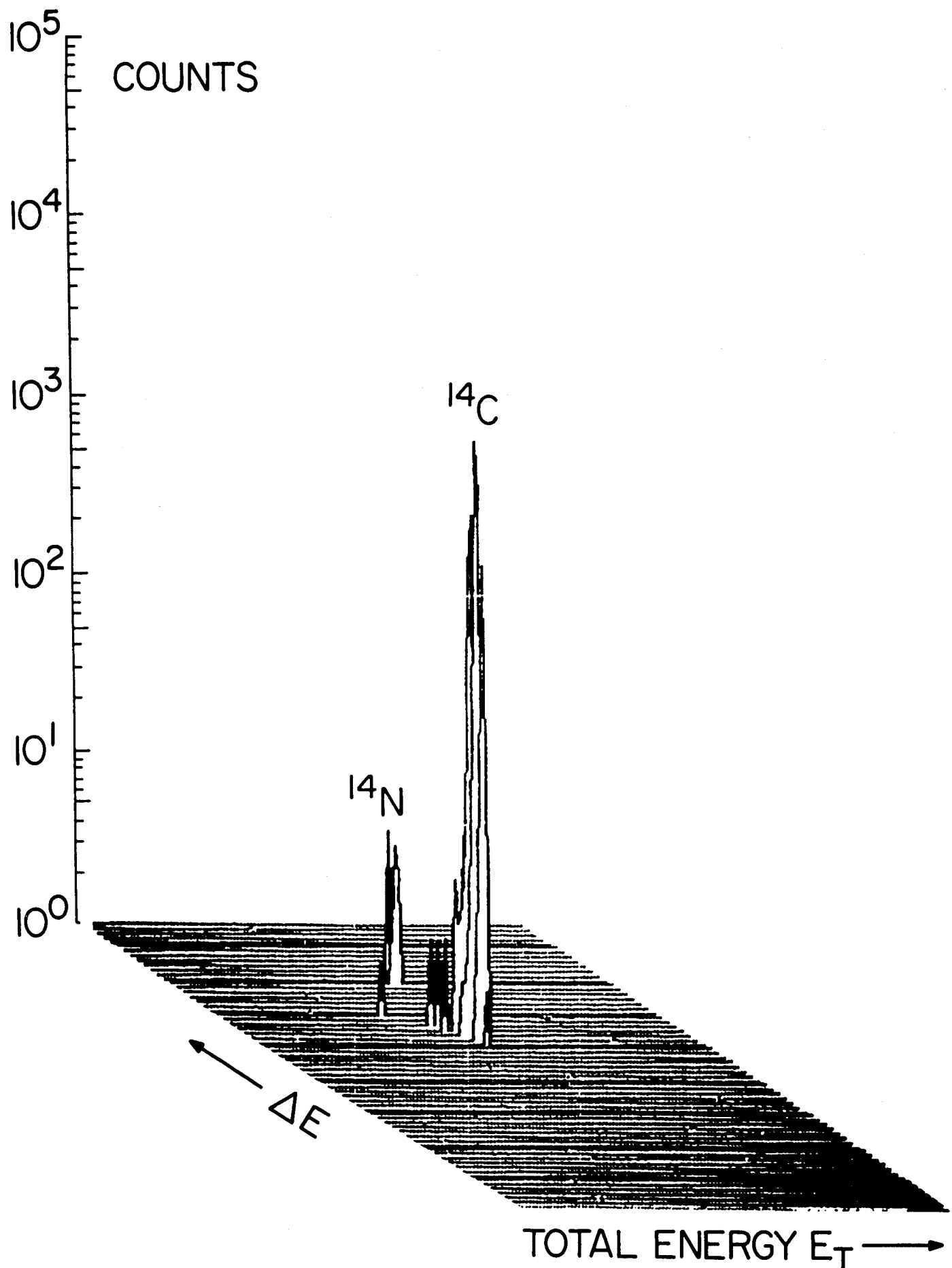


Fig. 2 A two parameter logarithmic plot of a spectrum obtained with the  $\Delta E$ -E heavy ion counter. The sample was modern carbon with  $^{14}\text{C}/^{12}\text{C} = 1.2 \cdot 10^{-12}$

be determined with an accuracy of 1%. Only 1 mg carbon is needed for such a measurement.

Presently the facility is used to date ice cores from Dye3, Greenland by measuring the  $^{14}\text{C}/^{12}\text{C}$  ratio of the  $\text{CO}_2$  trapped in the ice and to determine the  $^{10}\text{Be}$  activities of the same samples. The long living  $^{10}\text{Be}$  ( $t_{1/2} = 1.6 \cdot 10^6 \text{ y}$ ) is well suited to study variations in the interaction of the cosmic radiation with the atmosphere.

#### References

- {1} M. Suter, R. Balzer, G. Bonani, W. Wölfli  
IEEE Transaction on Nuclear Science NS-28, 1981, 1475
- {2} M. Suter, R. Balzer, G. Bonani, Ch. Stoller, W. Wölfli  
Proceedings of the Symposium on Accelerator Mass Spectroscopy,  
Argonne, 11-13.5.1981

### III. Eidg. Institut für Reaktorforschung, Würenlingen

#### 1. Charge distribution in the reactor-neutron-induced fission of $^{232}\text{Th}$

H.N. Erten, A. Grütter, E. Rössler, H.R. von Gunten

The independent yields of  $^{82}\text{Br}$ ,  $^{86}\text{Rb}$ ,  $^{96}\text{Nb}$ ,  $^{98\text{m}}\text{Nb}$ ,  $^{128\text{g}}\text{Sb}$  and  $^{136}\text{Cs}$  were determined in the reactor-neutron-induced fission of  $^{232}\text{Th}$  using radio-chemical techniques and  $\gamma$ -ray spectroscopy. The results are given in the following table:

$^{82}\text{Br}$	$(2.3 \pm 2.3) \times 10^{-4} \%$
$^{86}\text{Rb}$	$< 3.8 \times 10^{-4} \%$
$^{96}\text{Nb}$	$< 4.2 \times 10^{-5} \%$
$^{98\text{m}}\text{Nb}$	$(2.48 \pm 0.53) \times 10^{-3} \%$
$^{128\text{g}}\text{Sb}$	$(2.34 \pm 0.37) \times 10^{-3} \%$
$^{136}\text{Cs}$	$(1.70 \pm 0.13) \times 10^{-4} \%$

Using the extended  $Z_p$ -model of Wahl {1} with the yield data from this work and those for  $^{91}\text{Kr}$ ,  $^{131\text{p}}\text{Sn}$ ,  $^{131}\text{Te}$ ,  $^{135}\text{I}$  and  $^{140}\text{Xe}$  from the literature, the following parameters were obtained for the charge distribution in the reactor-neutron-induced fission of  $^{232}\text{Th}$ : Width of Gaussian charge dispersion  $\bar{\sigma}_Z = 0.52 \pm 0.01$  and  $\Delta Z_p = Z_p - Z_{p, \text{UCD}} = 0.45 \pm 0.02$ . The even-odd proton and neutron enhancement factors were found to be small.

#### Reference

{1} A.C. Wahl, J. Radioanal. Chem. 55(1980)111.

2. Decay data of  $^{81,82m,83,84m+g}\text{Rb}$  and  $^{83,85m,87m}\text{Sr}$

A. Grütter

In the course of cross section measurements in p-induced reactions we noticed that for some Rb- and Sr-isotopes major discrepancies exist between the  $\gamma$ -ray data of different authors, especially for  $^{81}\text{Rb}$  and  $^{84m+g}\text{Rb}$ . For  $^{82m}\text{Rb}$  and  $^{83}\text{Sr}$  the published data are scarce and have relatively large errors. For this reason we have determined half-life values and  $\gamma$ -ray energies and intensities for these and some other nuclides which were produced by bombarding several targets of RbCl with protons of different energies at the SIN-injector cyclotron. The targets differed considerably with respect to the radionuclides produced. Thus it was possible to choose the most suitable targets for the determination of the decay data, especially of the half-lives and the intensities of weaker  $\gamma$ -rays.

The evaluated half-life values are presented in the following table. The errors quoted for our results are statistical and represent 1 SD. Our results agree in general with the published half-lives. The accuracy has been improved for  $^{82m, 84m}\text{Rb}$  and  $^{83}\text{Sr}$ .

Nuclide	Half-life values	
	this work	literature values
$^{81}\text{Rb}$	$4.565 \pm 0.009 \text{ h}$	$4.582 \pm 0.009 / 4.575 \pm 0.0035$
$^{82m}\text{Rb}$	$6.472 \pm 0.006 \text{ h}$	$6.2 \pm 0.5 / 6.3 \pm 0.5$
$^{84m}\text{Rb}$	$20.26 \pm 0.04 \text{ min}$	$21.2 \pm 0.5 / 20.6 \pm 0.8 /$ $20.0 \pm 0.5 / 20.5 \pm 0.2$
$^{83}\text{Sr}$	$32.41 \pm 0.03 \text{ h}$	$31.4 / 32.4 \pm 0.2 / 32.9$
$^{85m}\text{Sr}$	$67.55 \pm 0.07 \text{ min}$	$67.66 \pm 0.07 / 67.92 \pm 0.25 /$ $67.3 \pm 0.3 / 68.0 \pm 0.2$
$^{87m}\text{Sr}$	$2.795 \pm 0.013 \text{ h}$	$2.81 \pm 0.02 / 2.830 \pm 0.010 /$ $2.793 \pm 0.009 / 2.805 \pm 0.003$
$^{34m}\text{Cl}$	$31.98 \pm 0.05 \text{ min}$	$32.06 \pm 0.08 / 31.99 \pm 0.05$

The  $\gamma$ -ray energies and relative intensities which we have found for the isotopes  $^{81}\text{Rb}$ ,  $^{82\text{m}}\text{Rb}$ ,  $^{83}\text{Rb}$ ,  $^{84}\text{Rb}$ ,  $^{84\text{m}}\text{Rb}$ ,  $^{83}\text{Sr}$  and  $^{85\text{m}}\text{Sr}$  are not quoted here. These values will soon be published in the International Journal of Applied Radiation and Isotopes. Especially in the case of  $^{82\text{m}}\text{Rb}$  and  $^{83}\text{Sr}$  the accuracy of the data has been improved appreciably and for  $^{83}\text{Sr}$  some additional  $\gamma$ -rays of very low intensity have been found. However, further information is still needed to clarify some uncertain and ambiguous placements in the decay schemes.

### 3. Fast neutron dosimetry of spallation sources

F. Hedegüs

The Swiss Institute for Nuclear Research (SIN) is building a spallation neutron source [1]. The principle is the following: in a cylindrical liquid-heavy-metal (Pb/Bi) target bombarded by a 590 MeV proton beam ( $\sim 1\text{ mA}$ ), fast neutrons with energies of a few MeV are produced. In the  $\text{D}_2\text{O}$  moderator, which surrounds the target, the fast neutrons are slowed down to thermal energies.

For the purpose of a fusion first wall material damage simulation, the intense fast neutron field could be of interest. The suitability of a spallation neutron source for this purpose depends mainly on the magnitude of the integrated fast neutron flux ( $E_n > 0.1\text{ MeV}$ ) and on the shape of the neutron spectrum. For this reason, fast neutron flux and spectrum measurements were performed at several possible locations around a mock-up target at the SIN accelerator.

The spallation source mock-up consisted of a cylindrical lead target ( $d = 15\text{ cm}$ ,  $l = 60\text{ cm}$ ) which was bombarded with a low current ( $1.0\text{ nA}$ ) proton beam of 590 MeV. The incident beam was along the axis of the cylindrical target which was surrounded by a  $\text{D}_2\text{O}$  moderator. The fast neutron flux measurements were done in two empty channels ( $d = 10\text{ cm}$ ) leading to the target. The channels have traversed the  $\text{D}_2\text{O}$  tank just below the target channel. The angle between the beam direction and the channel axis was  $90^\circ$



and  $150^\circ$ . It was assumed that the maximum fast neutron intensity point (point source) is at a depth of 10 cm from the front side of the target. Both channel axes were 13 cm below this point.

In order to measure in situ the fast neutron spectrum, the multi-foil threshold activation method was used. Detector sandwiches containing 7 foils each, were located at 9 different measuring positions. Parasitic activation due to thermal neutrons was reduced by covers of cadmium sheets. The induced activities were measured by means of a Ge(Li)-gamma spectrometer, in the case of induced X-ray activities a pure Ge detector was used. The reaction rates were calculated from the measured activities by using the nuclear constants given in {2}. The unfolding code SAND, with the cross section library of Greenwood {3}, was used to evaluate the neutron spectra. Time-of-flight spectra measured by KfK at SIN {4} and by LASL at LAMPF {5} were used as input spectra for SAND. It was found that the resulting spectrum for neutron energies below 30 MeV is practically independent of the input spectrum.

These investigations have shown that the SIN spallation neutron source could be useful for fusion first wall material studies provided that:

- the location of the material samples would be situated at least 10 cm from the assumed point source
- the proton current would be at least 1.5 mA.

If these conditions are satisfied, the neutron flux ( $E_n > 0.1$  MeV) will be  $\sim 6 \cdot 10^{13}/\text{cm}^2\text{sec}$  in the position of the material samples. During 3-4 months irradiations, significant production of helium gas and atomic displacements could be achieved.

#### References

- {1} W. Fischer, NEANDC (OR) - 152L, Part B (1979) 26
- {2} W.L. Zijp and J.H. Baard, ECN-70 (1979)
- {3} L.R. Greenwood, ANL/FPP/TM-115 (1978)
- {4} S. Cierjacks, M.T. Rainbow, M.T. Swinhoe and L. Buth, KfK 3079 B (1980)
- {5} R. Dierckx, private communication (1980)